Earth Surface Processes and Landforms
Earth Surf. Process. Landforms **24**, 71–90 (1999)

TECHNICAL COMMUNICATION

SEGMENTATION OF SOIL ROUGHNESS PROFILES

LORENZO BORSELLI*

CNR-IGES, Institute for Soil Genesis and Ecology Piazzale delle Cascine 15, 50144 Florence, Italy

Received 7 October 1997; Revised 17 June 1998; Accepted 7 September 1998

ABSTRACT

A robust and flexible algorithm to study spatial series like soil roughness profile has been introduced. It avoids using classic spectral analysis, considers the profile first and foremost as non-stationary and makes it possible to identify the separate domains inside the profile where chosen statistical parameters and roughness indexes have their own value. The method analyses a roughness profile considering it as an assemblage of several entities that may differ in terms of statistical properties and length, without establishing constraints as to number and extension. The method derives the variability of statistical and roughness properties along the profile and extracts the possible components – random and oriented – detectable inside the sample. Some examples of application illustrate the possibility offered by the method to study real roughness profiles recorded in the field by a portable laser microprofilometer. The procedure proposed allows the investigation of local roughness properties with varying degrees of accuracy and should be useful to monitor the differential evolution of roughness on patterned soil surface, increasing the overall information content. A general definition of 'ordered roughness' is introduced. The definition proposed seems more suited to current techniques for the numerical treatment of digital profiles and for the existing physical relationships between the scale of observation of roughness and the scale of the process investigated (hydraulic resistance, water storage in depressions).

KEY WORDS random roughness; oriented roughness; soil roughness profile; ordered roughness; segmentation

INTRODUCTION

Surface roughness influences soil hydrologic response and erosion through its interrelationships with hydraulic resistance (Gilley and Finkner, 1991), depression storage (Onstad, 1984; Linden *et al.*, 1988), and structural stability of the aggregate exposed to rainfall and runoff generation.

Soil surface roughness is the result of human-induced events and natural processes such as soil tillage and compaction, soil erosion and deposition, structural degradation of soil surface due to raindrop slacking and sealing process. Thus different types of roughness exist as a direct consequence.

Romkens and Wang (1986) recognized four different types of surface roughness, each one with a different order of magnitude: (1) microrelief variations due to individual or aggregate grains; (2) surface variation due to cloddiness; (3) difference in elevation due to furrows; and (4) higher-order roughness elevation variation at field basin or landscape level. The first two kinds of roughness are uniformly distributed in all directions and are usually referred to as random roughness. The third is often referred to as oriented roughness because it extends unidirectionally over the entire field (Allmaras *et al.*, 1966). In material sciences a clear distinction was also made between roughness superimposed over possible waviness present on the surface (Whitehouse, 1994).

Soil roughness is commonly measured in the field using contact (Kuipers, 1957; Burwell *et al.*, 1963) or non-contact profilometers, the latter based on laser beam devices (Huang *et al.*, 1988, 1992; Bertuzzi *et al.*, 1990a). The soil surface is then described by matrices containing the elevation measurements and their relative position usually measured at constant intervals on the horizontal plane (surface representation) or line (transect representation).

* Correspondence to: Dr L. Borselli, CNR-IGES, Institute for Soil Genesis and Ecology, Piazzale delle Cascine 15, 50144 Florence, Italy

CCC 0197-9337/99/010071–20 $17.50

For the past three decades growing attention has been given to the quantitative characteristics of soil roughness. Several authors have reviewed and proposed various indexes of soil surface (Linden and van Doren, 1986; Zobeck and Onstad, 1987; Lehrsch *et al.*, 1988; Bertuzzi *et al.*, 1990b). The most well-known in soil science are: random roughness (RR) (Kuipers, 1957; Allmaras *et al.*, 1966; Currence and Lovely, 1970) defined as the standard deviation of the detrended elevation measure; AF index (Romkens and Wang, 1986,1987); LS and LD indexes (Linden and Van Doren, 1986); tortuosity index (R) (Bertuzzi *et al.*, 1990b); and fractal dimension (Andrle and Abrahams, 1989), Perfect and Kay 1995; Gallart and Pardini, 1996). All these indexes are calculated starting from the digitized surface or transect profile at constant intervals.

Other common techniques of analysing digital roughness profiles are signal processing methods (Whitehouse, 1994). Spectral analysis of the roughness profiles was used for surface classification and quantification purposes (Stone and Dugundji, 1965; Green, 1967). Podmore and Huggins (1980) used spectral analysis to evaluate the hydraulic resistance properties of surfaces. Destain *et al.* (1989) used spectral analysis to quantify seasonal degradation of small-scale roughness associated with small clods on a fresh tilled surface. Frede and Gath (1995a, b) used spectral analysis to derive the dimensional distribution of clods and aggregate on the top of the surface. Spectral analysis is affected by several problems, mainly the difficulty of revealing frequencies higher than the 'cut-of Nynquist frequency' caused by the sampling distance and the possible bias that may affect the power spectrum due to 'aliasing' or to modifications produced by high frequencies on low-frequency amplitudes (Green, 1967).

Soil roughness is not static but changes with time, depending on soil characteristics and the succession and intensity of the events causing its generation or degradation (Dexter, 1977; Zobeck and Onstad, 1987). A general decay of roughness indexes was usually observed with the increase of cumulative rainfall or cumulative kinetic energy applied (Zobeck and Onstad, 1987; Potter, 1990; Van Wesmael *et al.*, 1996). Most roughness decay models follow a negative exponential trend and usually the model parameters (e.g. decay velocity) were related to soil properties such as clay content (Potter, 1990), but were also influenced by rock fragment content (Van Wesmael *et al.*, 1996).

Sampling lag influences the scale of roughness that can be revealed and thus has considerable effect on the computed roughness. This is the case of the fractal dimension D computation (Andrle and Abrahams, 1989; Gallart and Pardini, 1996), and the influence on some direct determinations such as surface water storage in the depression (Brough and Jarret, 1992).

In all the studies cited above, the processing of roughness profiles was performed considering each one as a single entity defined by a roughness index representing its statistical properties.

Following this approach, where strong variability of roughness properties along the profile occurs, some of the existing roughness components may not be revealed and if different parts with a proper distinct roughness index exist they may be redistributed all along the profile and disappear in a sort of averaging so that the local properties and variability are lost. The loss of information affects the possibility of improving the assessment of local storage capacity, by statistical relationships (Onstad, 1984; Linden *et al.*, 1988) and its variability, as well as on the discrimination of existing roughness components and the possibility of analysing the differential evolution of separate parts under rainfall–runoff forces.

The strategies adopted in surface metrology (Whitehouse, 1994) constitute an alternative approach. One method subdivides the profile into equal length spans and evaluates local roughness indexes in each. In this way the information content derived is improved but a clear bias affects the procedure due to the choice of the segment lengths. The separation of components may be accomplished with common spectral analysis methods (Whitehouse, 1994; Hegge and Masselink, 1996) but where the signal has non-stationary properties (most general case) more complex methods are required and constant length partition and subsequent analysis is performed (Hegge and Masselink, 1996). Major difficulties arise if the roughness components are arranged in an irregular pattern along the profile. This is the most general case where the classic approaches encounter major problems.

In Figure 1a, b an ideal example of a profile is obtained by merging separate components. Figure 1a

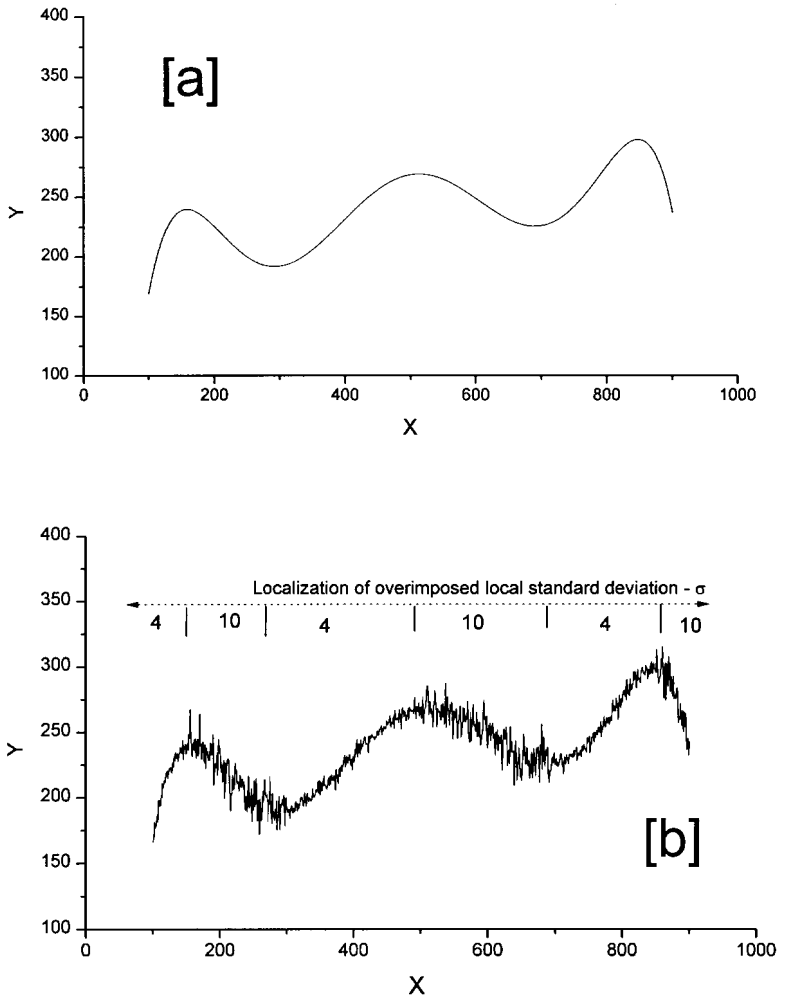

Figure 1. Drive example of roughness components distributed with spatial pattern and local variability along a profile: (a) roughness component produced by a sort of ridging; (b) the result of merging with smaller-scale roughness yielded by attaching three parts with different roughness components

shows the roughness component of a sort of ridging produced by a seventh degree polynomial superimposed over a linear trend. Figure 1b shows the result of merging with two smaller-scale roughness components, different in magnitude, with standard deviation of 4 and 10 respectively, on the two sides of the ridged structure. The example in some way resembles the case when the soil surface is exposed to wind-driven rainfall, producing a differential evolution on the leeward face roughness (Poesen, 1988; Torri, 1996). In this case evaluating roughness characteristics and evolution separately, on the existing different domains of the profile, may be very useful.

The study of a roughness profile may proceed in many ways. When aiming to determine the RR index, the simplest procedure is to try to identify an existing trend, remove it and thus calculate RR on the residuals. Figure 2a, b shows the results of two types of detrending processes applied to the profile in Figure 1 (e.g. linear and polynomial). The corresponding RR calculation based on the residuals of six-degree polynomial fitting (Figure 2b) is 7.28. Both the methods identify – with varying degrees of error – two components of the roughness: the oriented roughness, as linear or polynomial trend, random roughness, based on the respective residues. By increasing the degree of polynomial fitting the residuals,

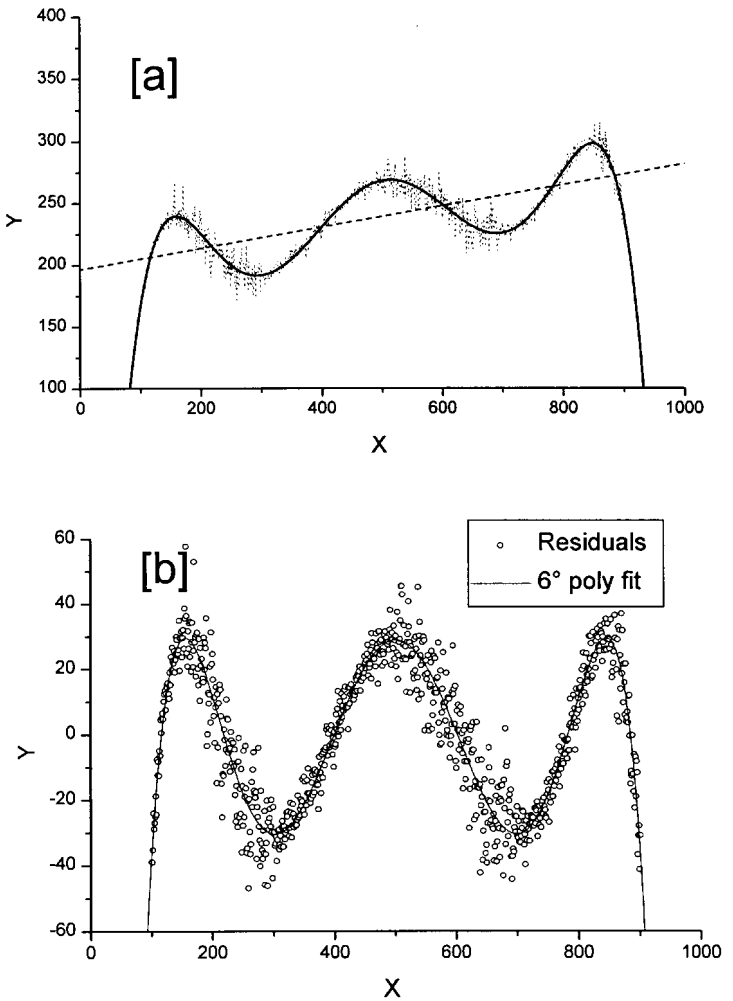

Figure 2. Results of two types of detrending process: linear and polynomial, and the corresponding RR (random roughness) calculation based on the residuals done on the drive example in Figure 1. Both methods identify two components of roughness with different degrees of error: (a) linear and polynomial detrending; b) residuals to calculate overall RR index

and thus random roughness, become negligible. Nevertheless no other type of information can be derived using these procedures because the roughness that exists locally (e.g. on the left and right side of the ridge) was averaged over the whole profile.

The application of standard spectral analysis in cases of non-stationary and non-periodical spatial series poses some problems as in Figure 1. The ridged profile in Figure 1 was previously linearly-detrended and then a common spectral analysis by Fast Fourier Transform (FFT) was applied. Figure 3a shows the derived power spectrum of the structure. The maximum value at period 400 that corresponds to the existing symmetry is evident. The superimposed roughness is not clearly represented as shown in the Figure 3b, c. Considering the entire profile, the lower-order roughness is not clearly identified by the spectrum in Figure3a and it is not clear how many spectral components are needed to reach a sufficient description of the profile.

An alternative procedure allows us to obtain a higher degree of information compared to that previously described: (1) by-eye partition of the profile; (2) separate analysis of roughness in each of the identified domains.

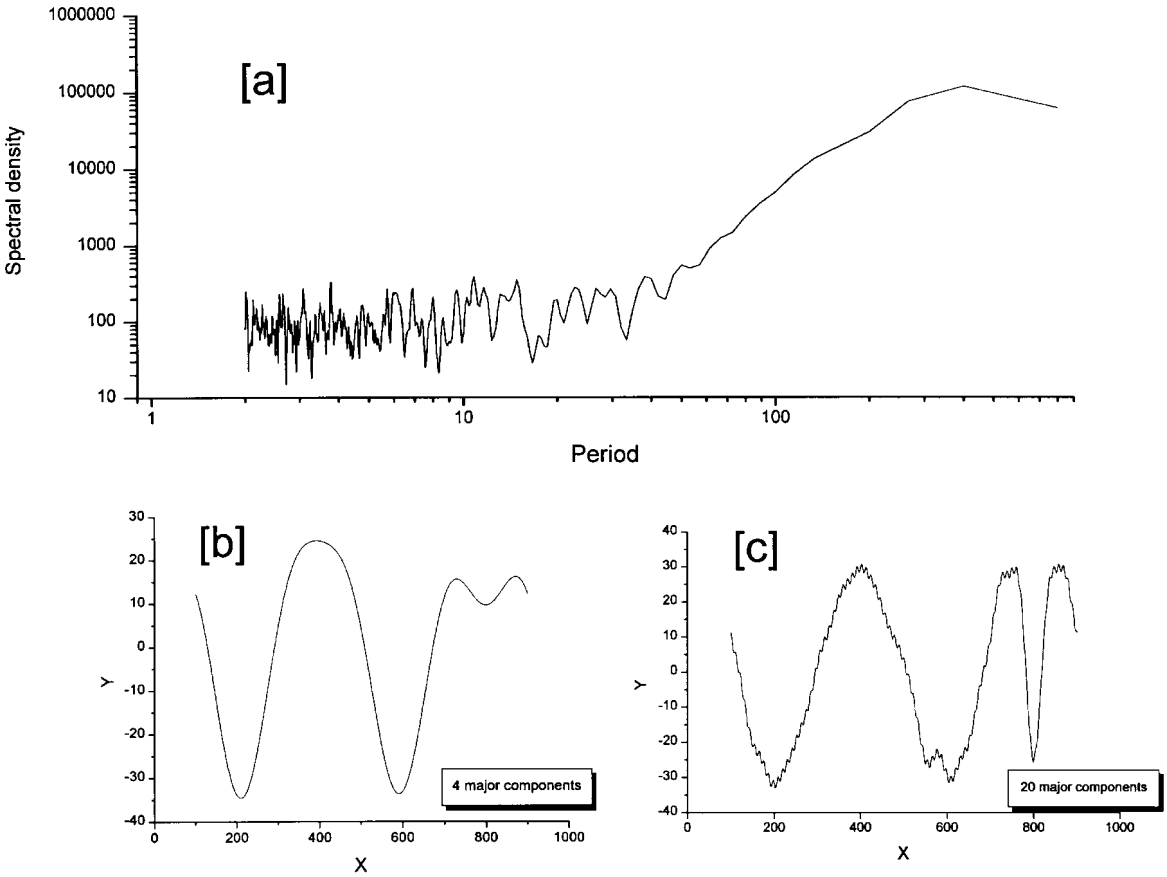

Figure 3. Spectral analysis of the profile in Figure 1: (a) power spectrum; (b) profile summing first four spectral components; (c) profile summing first 20 components.

By-eye partition and analysis of a profile is conceptually easy but extremely subjective, and not feasible in some complex cases (e.g. domains with fuzzy limits or with visually undetectable separate parts). But the more interesting type of information that can be extracted from a measured soil roughness profile is the discrimination of the profile itself into several parts that can be considered homogeneous in terms of certain properties such as: the average elevation, the same average local slope and the same degree of roughness. At the same time this type of information makes it possible to locally separate random from oriented roughness components.

The operation of locating regions that correspond to surfaces or objects in three-dimensional digital image processing leads to the subdivision of the image into a countable number of parts ('segmentation') that may be assumed to be homogeneous with respect to the given characteristics or properties. In this paper the same concept will be applied to two-dimensional space. In the case of soil roughness profile the previous definition of segmentation thus becomes 'the subdivision of the profile into parts with different roughness or statistical properties'.

The aim of this paper is to describe a new heuristic method for analysing soil roughness profiles, considering them as an assemblage of several entities that may differ in terms of statistical properties and lengths without assuming constraints on their number and extension. We also derived the variability of statistical and spatial roughness properties along the profile, extracting the possible components detected inside the sample.

THE SEGMENTATION ALGORITHM

The algorithm applies to all kinds of roughness profiles irrespective of their resolution and number of points, without the use of spectral analysis. The algorithm, implemented in Object Pascal code, is based on the use of simple statistical indexes that correspond to several segmentation criteria able to identify the spatial distribution of certain characteristics along the profile.

The basic data structure consists of two unidimensional vectors that contain respectively: $\boldsymbol{X}$, the locations of n equally spaced elevation measures, and $\boldsymbol{Y}$, the corresponding elevation measures.

The algorithm makes extended use of a type of function that performs a simple transformation of vector $\boldsymbol{Y}$ producing a third vector $\boldsymbol{Z}$. The transformation function, called in this study *Tfunction*, is the basis for the segmentation process. Each *Tfunction* input the vectors $\boldsymbol{X}$ and $\boldsymbol{Y}$ as standard and the index i of the ith transformed value. As standard output each *Tfunction* produces a transformed value z_i corresponding to the ith location in the vector $\boldsymbol{Y}$. The *Tfunction* is called up iteratively for all the n elements stored in the $\boldsymbol{X}$ and $\boldsymbol{Y}$ vectors and calculating all the elements of the $\boldsymbol{Z}$ vector.

The general formalism adopted for a *Tfunction* is the following:

$$Tfunction = f([\boldsymbol{X},]\boldsymbol{Y},i) \tag{1}$$

Square brackets indicate that for some *Tfunction*s only the $\boldsymbol{Y}$ vector is required as input and

$$z_i\, f_i\, ([\boldsymbol{X},]\boldsymbol{Y},i) \tag{2}$$

A fourth vector $\boldsymbol{C}$ is then derived by calculating the cumulative values in vector $\boldsymbol{Z}$:

$$c_m = \sum_{i=1}^{m} z_i \tag{3}$$

where c_m is the mth element of the $\boldsymbol{C}$ vector, where $m \in [1...n]$..

The adopted *Tfunction*s are simple statistical or analytical functions listed in Table I. The segmentation algorithm studies the trend of the derived vector $\boldsymbol{C}$ by the iterative application of linear regression techniques and deriving, for this end, a new vector $\boldsymbol{R}$.

The ith member (r_i) of the vector $\boldsymbol{R}$, with $i \in [1...n]$, is computed using the following function:

$$r_i = p_i(\boldsymbol{X},\boldsymbol{C},i) \tag{4}$$

where p_i is the function that computes the coefficient of determination (r^2) of the linear regression related to the first i data points, at ith location of the $\boldsymbol{X}$ and $\boldsymbol{C}$ vectors.

The analysis of $R(i)$ function graph makes it possible to find the upper bound of the first segment of the profile. The successive segments in the profile are identified repeating the calculation of $\boldsymbol{C}$ and $\boldsymbol{R}$ vectors using the remaining part of the original profile that follows the upper bound of the previously defined segment. The process is repeated in this way until the entire profile is partitioned.

The process works with the following steps:

(1) starting from the first point in the profile ($i = 1$) vectors $\boldsymbol{C}$ and $\boldsymbol{R}$ are generated with Equations 3 and 4;
(2) at the first iteration the lower bound of the first segment is fixed at element $i = 1$ of the vector;
(3) the upper bound of the segment is established looking at the trend of the derived $R(i)$ function graph (Figure 4); vector $\boldsymbol{R}$ was searched to find the index with the highest relative maximum value that follows its absolute minimum (Figure 4);

Table I. List of *Tfunctions* used as criteria for the roughness profile segmentation process

Name	*Tfunction*	Notes
SLOPE	$f_i = \dfrac{i\sum_{j=1}^{i} X_j Y_j - \sum_{j=1}^{i} X_j \sum_{j=1}^{i} Y_j}{i\sum_{j=1}^{i} X_j^2 - \left(1\sum_{j=1}^{i} X_j\right)^2}$	Slope of the standard linear regression applied to the indicated portion of the measured data set.
AVERAGE	$f_i = \dfrac{\sum_{j=1}^{i} Y_j}{i}$	Forces zones to be found where the average elevation remains at least uniform.
STDDEV	$f_i = \sqrt{\dfrac{i\sum_{j=1}^{i} Y_j^2 - \left(\sum_{j=1}^{i} Y_j\right)^2}{i(i-1)}}$	Forces zones to be found where the standard deviation of the elevation measurements is uniform.
SMALL SLOPE	$f_i = \dfrac{Y_i - Y_{i-1}}{X_i - X_{i-1}}$	First local derivative calculated numerically as backward difference. In this case we obtain C = Y.
NONE	$f_i = Y_i$	Does not perform any type of transformation on vector *Y*. *C* is obtained as the simple progressive accumulation of elevation measurements.

(4) the upper bound of the first segment is located in the highest relative maximum so found;
(5) if the upper bound found does not coincide with the last element of vectors ***X*** and ***Y*** the above procedure (steps 1 to 4) is iterated, calculating new ***C*** and ***R*** vectors on the remaining part of ***X*** and ***Y*** data vectors, that contain the information of the original profile, and identifying all the remaining segments in the same way.

The study of function $R(i)$ in Figure 4 identifies the extension of the straighter part of vector ***C*** which corresponds to the part where the criteria used for segmentation (e.g. average local slope, average elevation, etc.) can be reasonably taken as constant.

The segmentation process described above identifies the various parts of the profile without first establishing a constant partition length but has to be considered an adaptive process using variable length.

A second action may be opted for just after the basic segmentation process is terminated. Segments with lengths shorter than the predefined value are rejected and joined to the adjacent segments.

When the segmentation process is completed, the successive phase is to process the information content inside each segment or part of the original profile. Basic statistical parameters related to each segment identified by indexes a and b – the lower bound and the upper bound, respectively – of original data vectors ***X*** and ***Y*** are calculated with the values in the interval $[a,b]$: average elevation, standard deviation, local slope (by linear fitting of the data in each segment with a straight line), the residuals and

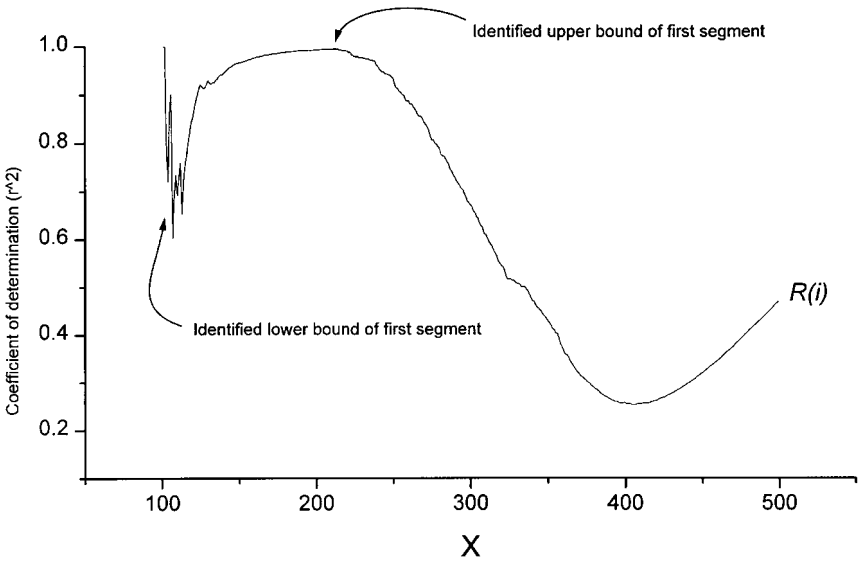

t-Figure 4. Search of the upper bound of a profile segment looking at the trend of function $R(i)$ computed by Equation 4

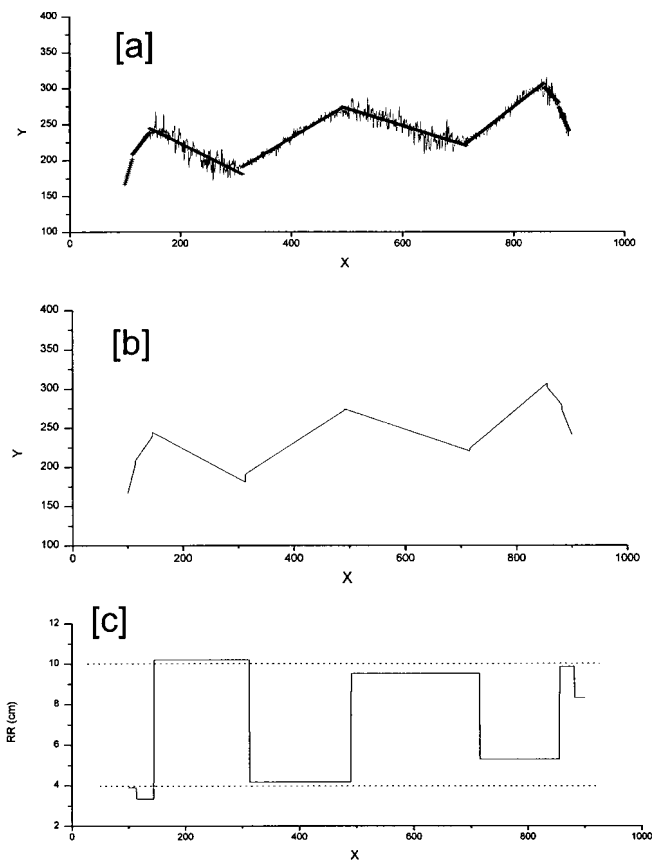

Figure 5. Application of the segmentation algorithm proposed to the drive example: (a) identification of high-order roughness produced by the ridge using SLOPE criterion; (b) profile approximation with higher-order roughness component; (c) spatial distribution of identified local RR index

he standard deviation of the residuals of the linear fitting (RR), AF roughness index of the residuals with respect to a local straight-line fitting.

Various indexes of roughness (RR, AF) may be calculated in distinct parts of the profile but also a new profile may be created by combining the local residues or local slope trend lines.

The result of the application of the algorithm to the drive profile in Figure1 is shown in Figure 5. Using SLOPE *Tfunction* as segmentation criteria, the profile is partitioned considering the local slope trend. When deriving a new profile by combining the straight lines obtained by local linear fitting in each segment, a higher class of roughness is obtained (see Figure 5a, b). A spatial distribution of the roughness parameter RR may be obtained by plotting the standard deviation of the local residuals of the local linear fitting (Figure 5c). The algorithm gives a good approximation of the original ridged structure and the different roughness components superimposed at the two sides of the ridges.

EXAMPLES OF APPLICATIONS

Profiles collected in two different localities are used as practical examples of application of the method proposed.

Materials and methods

The profiles were collected in late autumn 1996 at two locations in the central hilly region of Tuscany (Italy) using a portable laser scanner microprofilometer with maximum vertical and horizontal resolution of 0·5 mm, which is an improved version based on a previous device (Pini *et al.*, 1995). The first set of profiles (S. Gimignano site) was collected in a field with prevailing sandy loam soils after an intense erosive storm in autumn 1996. The second set of profiles (Vicarello site) was collected in spring 1997 from a fresh-disked surface with an average slope of 15–20° on a clay loam soil. Every profile in the set was collected using constant horizontal spacing of the measure of 1 mm with lengths ranging from 800 to 1400 mm. The main characteristics of the profile in the examples and the *Tfunction* used in the application of the segmentation algorithm are given in Table II. After the application of segmentation algorithms some roughness indexes are computed in each identified domain inside the profiles: the random roughness (RR), according at the definition of Currence and Lovely (1970), and, in some cases, the composite index AF, the product of microrelief index and frequency of peaks, in the same way as defined by Romkens and Wang (1986).

Description and analysis of the profiles

The first example in Figure 6 (S. Gimignano 1) came from a large interrill area. The algorithm identifies two separate portions on the profile that have different orientations of local slope as shown from the identified local linear trend. In the processing a minimum segment length of 10 cm was previously assumed. Computed in relation to the local linear trend identified, the local residuals in each part were analysed to obtain the values of local roughness index: RR and AF. By applying a standard

Table II. Characteristics of the profiles used on the application examples and *Tfunctions* used in the analysis

Profile name	Features	*Tfunction* used	Notes
S. Gimignano 1	Large interrill area	SMALL-SLOPE	
S. Gimignano 2	Large-shallow rill	SMALL-SLOPE	
S. Gimignano 3	Rill + side interrill area	SMALL-SLOPE	
Vicarello 1	Fresh-disked surface across slope	AVERAGE	Profile recorded across slope
Vicarello 2	Fresh-disked downslope	SLOPE	Profile recorded downslope
Vicarello 3	Fresh-disked downslope	SLOPE	Profile recorded downslope

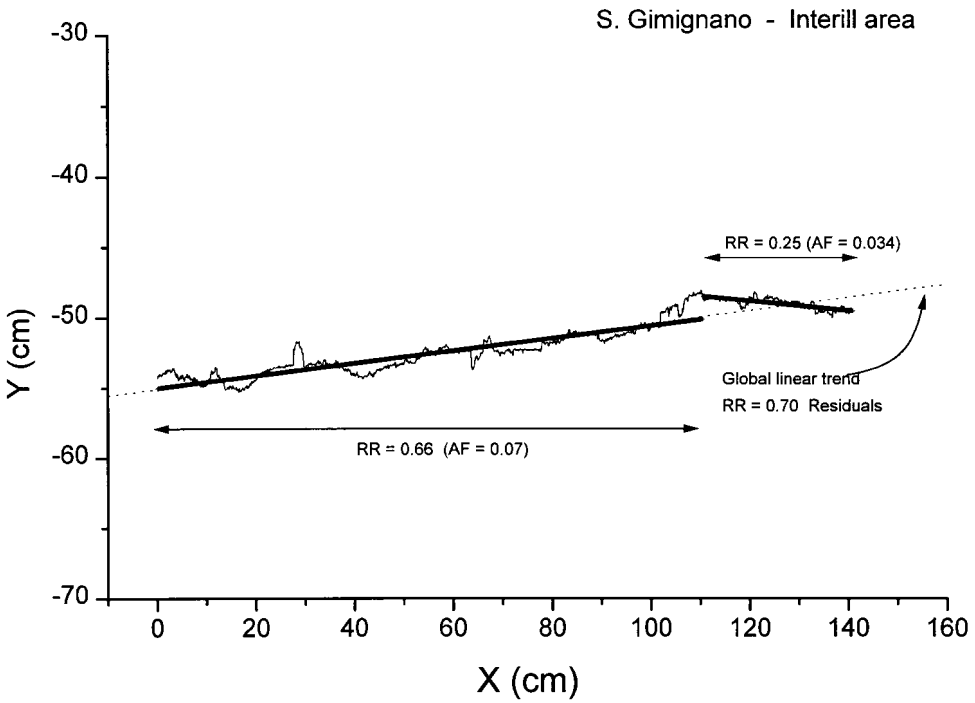

Figure 6. Application of the algorithm to the S. Gimignano 1 profile, representing an interrill surface. Local RR and AF roughness indexes

linear detrend on the entire profile the RR of residuals becomes higher than the RR obtained for the two parts identified by the segmentation algorithm. Global linear detrend is unable to detect the roughness feature and local slope of the second and smaller part. This example demonstrates the loss of information linked to the standard method of analysis.

The profile in Figure 7a (S. Gimignano 2) includes a wide and shallow rill. The algorithm identifies the local linear trend at the sides of the rill bottom (Figure 7b). The spatial distribution of the standard deviation of the residuals, calculated in relation to the local linear trend identified along the profile, is shown in Figure 7c.

Using the same *Tfunction* the algorithm was applied to the third profile taken at the S. Gimignano site (S. Gimignano 3). The profile represents a deep and narrow rill with a large surrounding interrill area (Figure 8a). The algorithm discriminates the interrill areas from the rill sides and bottom (Figure 8b). The distribution of the standard deviation of the residuals in relation to the local linear trend identified along the profile is shown in Figure 8c. The interrill areas have quite the same RR, while the major differences are the local slopes in each part detected.

The profiles in Figures 9, 10 and 11 were collected at the Azienda Agricola S. Elisabetta (experimental farm) (Vicarello). The profile in Figure 9a (Vicarello 1) was recorded by positioning the transect line across the main slope. The central depression of the profile corresponds to one of the tracks of the tracklayer tractor. The segmentation process identifies the limits of the track where both the fragmentation of the tracklayers and the effect of the disks act. The central part has a lower roughness compared to the sides (Figure 9b and 9c). The profile in Figures 10a (Vicarello 2) and 11a (Vicarello 3) are taken along the main slope of the field and a different *Tfunction* was used to consider the local and general trend of the slope. The profile in Figure 10a was measured between the track strips. The local and general slope trend is shown in Figure 10b. The spatial distribution of the local residuals' standard deviation is given in Figure 10c. The analysis is repeated in the same way for the profile in Figure 11 that was taken from the adjacent strip where the track was run down.

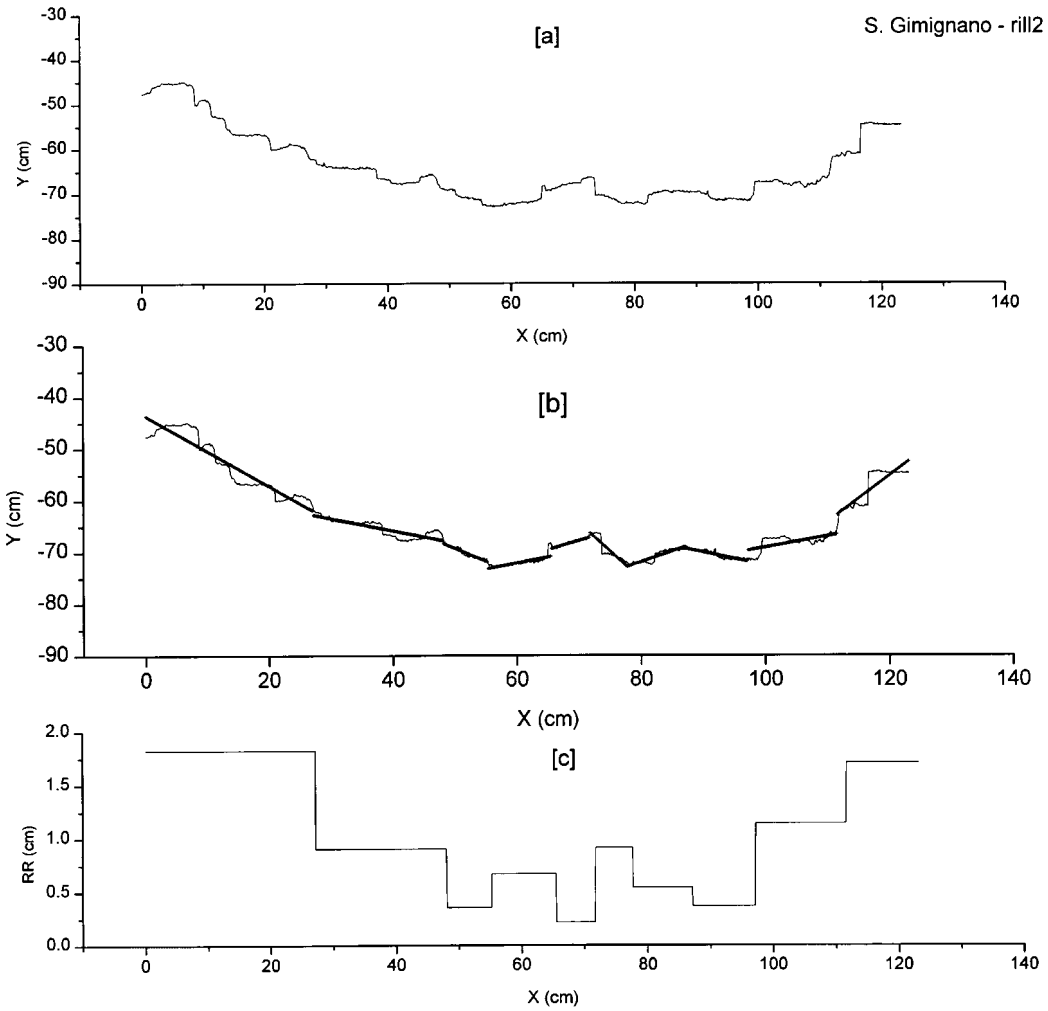

Figure 7. Application of the algorithm to S. Gimignano 2 profile, representing a wide and shallow rill profile: (a) original profile; (b) segmentation and identification of local linear trend; (c) spatial distribution of RR index

Figures 10c and 11c show the differences in roughness magnitude of the two profiles after the effect of the slope was removed locally.

The spatial distribution of the roughness in Figures 9c, 10c and 11c may be rearranged taking into consideration the frequency of a given roughness value in terms of its relative presence on the entire profile length. In this manner a cumulative density function (CDF) of roughness index may be established for every profile as is shown in Figure 12.

The main difference in the roughness statistical properties of profiles in Figures 9a, 10a and 11a is stressed by Figure 12. The Vicarello 2 and Vicarello 3 profiles represent long samples of roughness for each of the features presented in the disked surface along the main slope direction and the difference in the magnitude of this roughness is shown by the respective CDF of the roughness index. The Vicarello 1 profile shows the two features in the same profile even if they can be distinguished by the algorithm. The difference in the roughness magnitude in the Vicarello 1 profile (Figure 9) compared to Vicarello 2 and Vicarello 3 (Figures 10 and 11) may be explained by the fact that some long and narrow clods produced

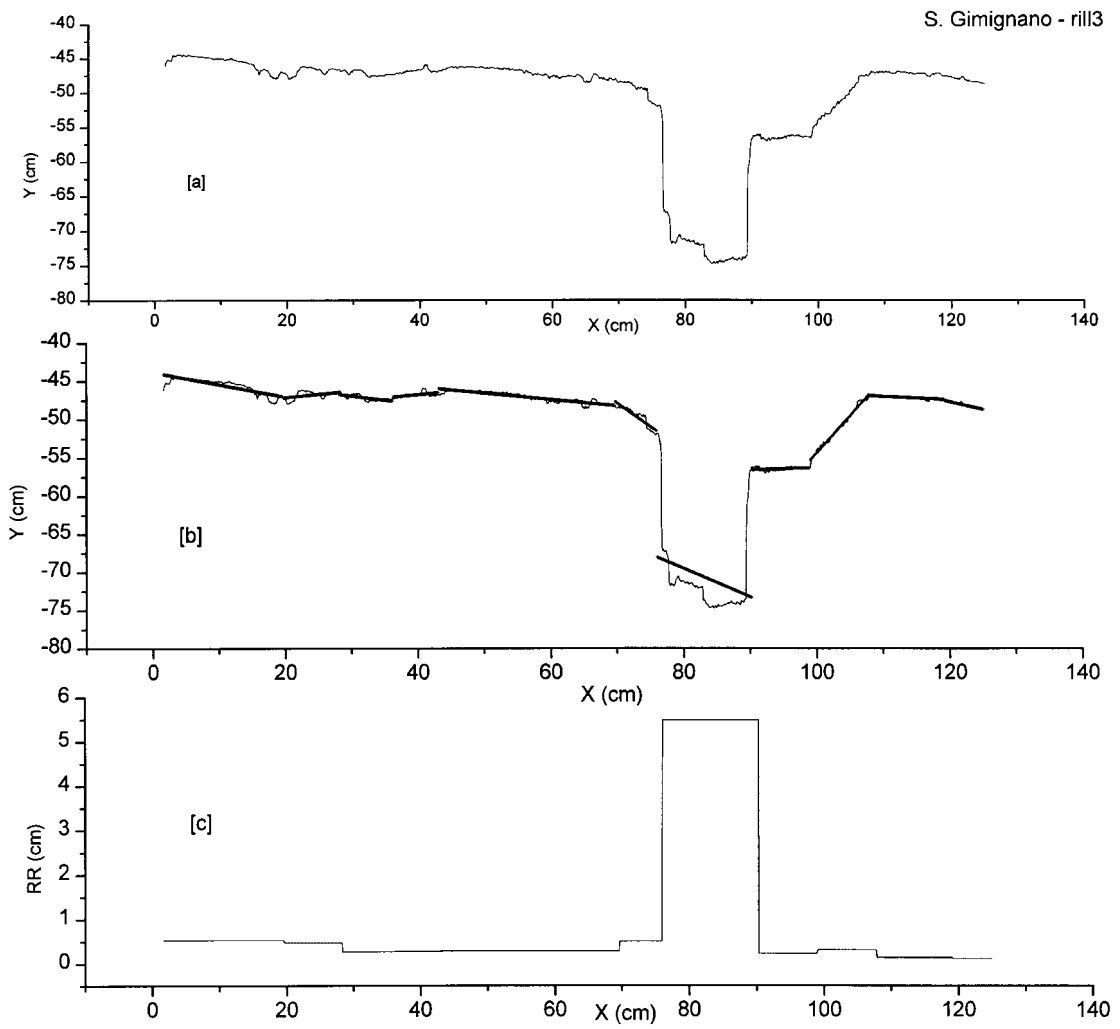

Figure 8. Application of the algorithm to S. Gimignano 3 profile, representing a deep rill with sloping sides and surrounding interrill areas: (a) original profile; (b) segmentation and identification of local linear trend; (c) spatial distribution of RR index

by the disk action are mainly arranged with their long axis oriented down-slope so that an across-slope profile clearly highlights the effect that the narrow step sides of these clods have in amplifying the roughness.

ORDERED AND PERIODIC COMPONENT EXTRACTION

The ability of the proposed algorithm to separate the superimposed RR over higher-order roughness was tested for the capacity to reveal the periodicity on some profiles partially masked from Gaussian noise.

Twelve profiles were created with different characteristics which are given in Table III. Each profile is characterized by 1000 elevation points equally spaced at 0·1 cm distance. Each signal was obtained by summing the mapped Sin(x) function with a different wavelength and unit amplitude to Gaussian noise

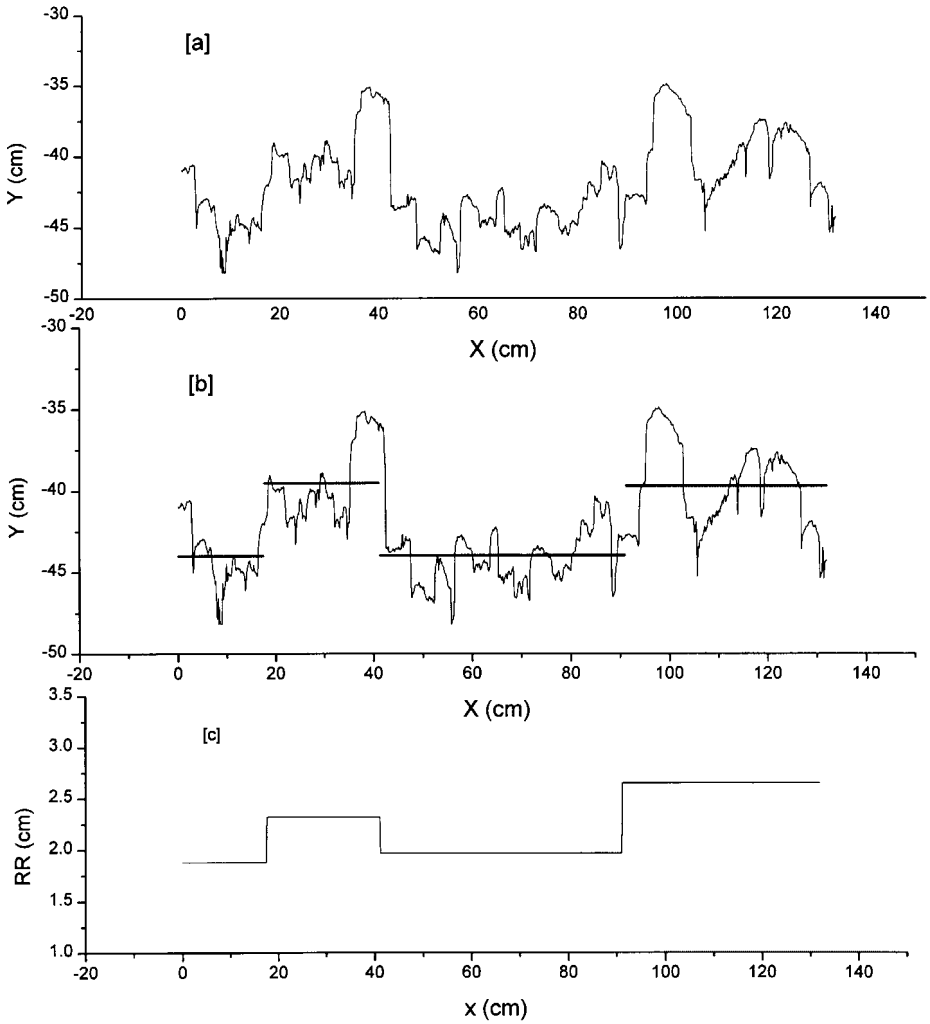

Figure 9. Application of the algorithm to Vicarello 1 profile, fresh-disked surface digitized across the main slope: (a) original profile; (b) segmentation with AVERAGE criterion, c) spatial distribution of RR index

with zero mean values and different standard deviation.

The segmentation criteria based on the SLOPE *Tfunction* were adopted for every profile test.

For each profile the test was repeatedly performed after resampling and increasing the lag from 1 to 10 points (0·1–1 cm). In this way the algorithm is applied to various combinations of sampling distance/period (ST) and with different Gaussian noise/base amplitude (NA), using the common base amplitude of 1 cm.

The algorithm performance is evaluated on the basis of the ability to identify the original noise and the base wavelength in each signal. The results are shown in Figures 13 and 14.

The steps of the simulation repeated for each profile are the following:

(1) load the profile data vectors;
(2) define the lag to use and resample the basic profile;
(3) compute the ST and NA rate;
(4) run the segmentation algorithm by extracting high-order and RR components from the profile;

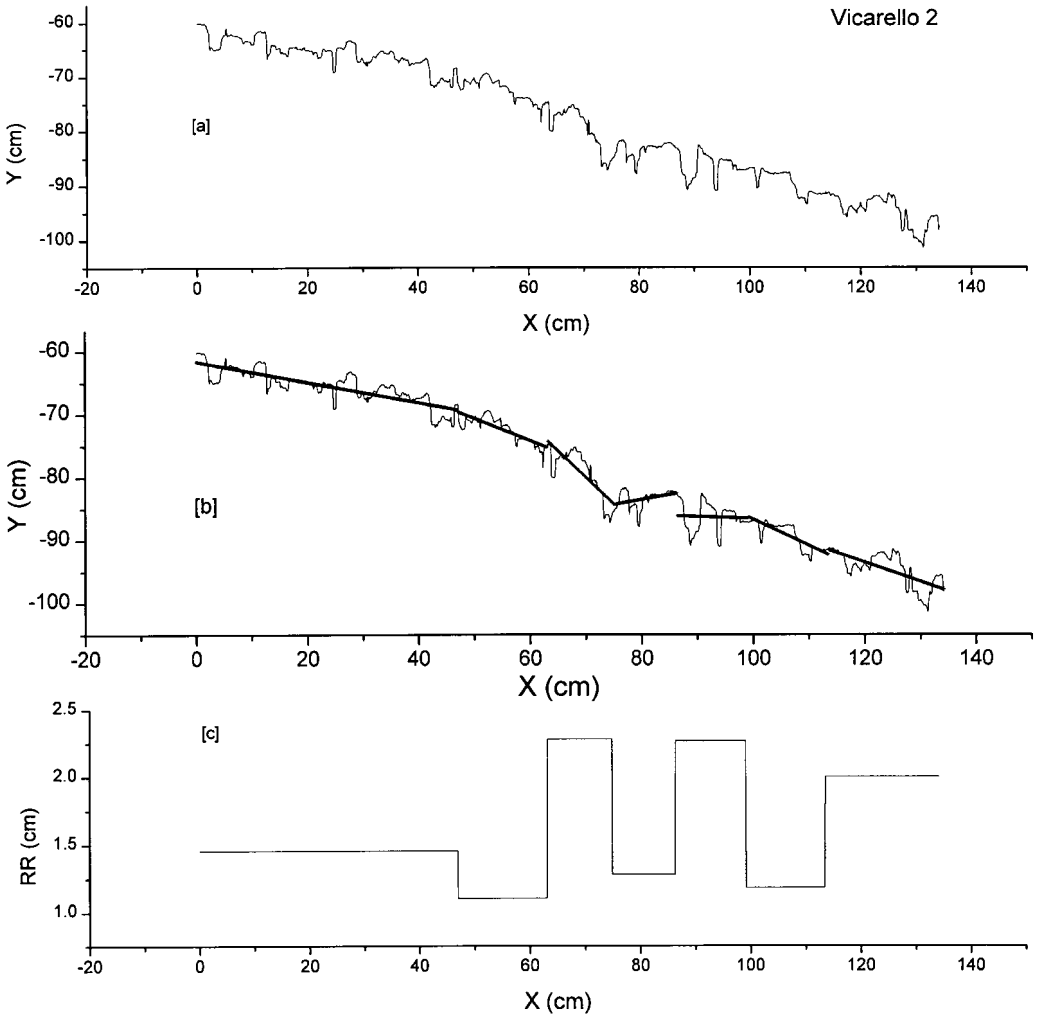

Figure 10. Application of the algorithm to Vicarello 2 profile, fresh-disked surface (inter-track strip) digitized downslope: (a) original profile; (b) segmentation and identification of local linear trend; (c) spatial distribution of RR index

(5) once the high-order roughness component is extracted, which is defined by combining all local slope trend segments, it is analysed with well known power spectral estimates MEM algorithm (Maximum Entropy Method or Burg method) (Press *et al.*, 1986) to define the main wavelength in a set of equally spaced data;
(6) the standard deviation on the RR component extracted, defined by the standard deviation on the local residue, is computed;
(7) the ratio between the main wavelength of the high-order roughness component extracted and the original wave length of the signal (ETT) is computed and plotted against the rate NA and ST (Figure 13);
(8) the ratio between estimated noise and original noise of the signal (ENN) is computed and plotted against NA and ST (Figure 14).

Considering the resampling process on the 12 different basic profiles the simulation was run 120 times. In the graphs in Figures 13 and 14 all the parameters involved are unidimensional. The graphs illustrate

Table III. Profile parameters used in the simulation. The profile is generated with a sine function with unit amplitude (1cm) and given period *T*. A Gaussian noise was summed at the base sine function

Profile no.	Gaussian noise (st dev.) (cm)	Period (T) (cm)
1	2	12·56
2	2	31·41
3	2	62·83
4	1·5	12·56
5	1·5	31·41
6	1·5	62·83
7	1	12·56
8	1	31·41
9	1	62·83
10	0·5	12·56
11	0·5	31·41
12	0·5	62·83

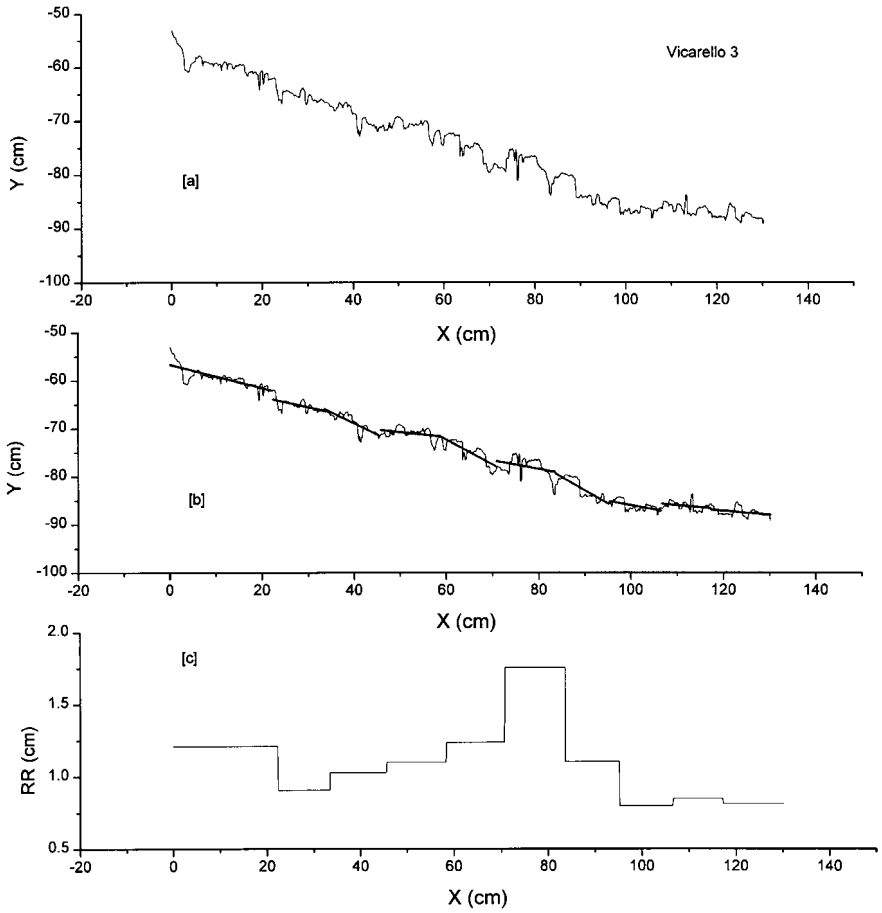

Figure 11. Application of the algorithm to Vicarello 3 profile, fresh-disked surface (track strip) digitized downslope: (a) original profile; (b) segmentation and identification of local linear trends; (c) spatial distribution of RR index

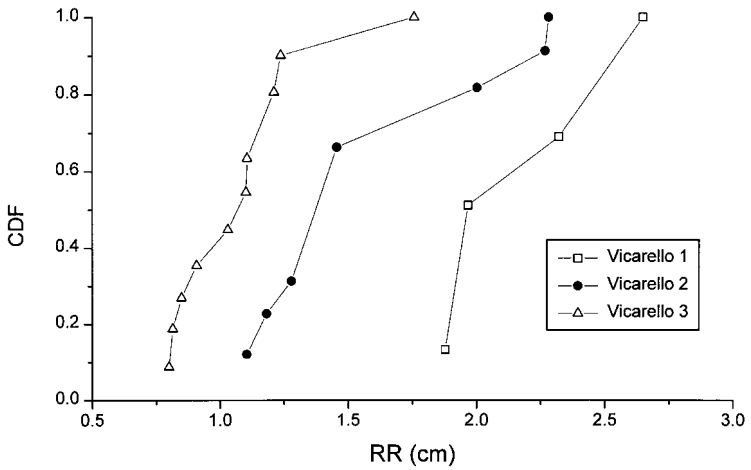

Figure 12. Cumulative density function (CDF) of the random roughness component for the profiles at Vicarello site

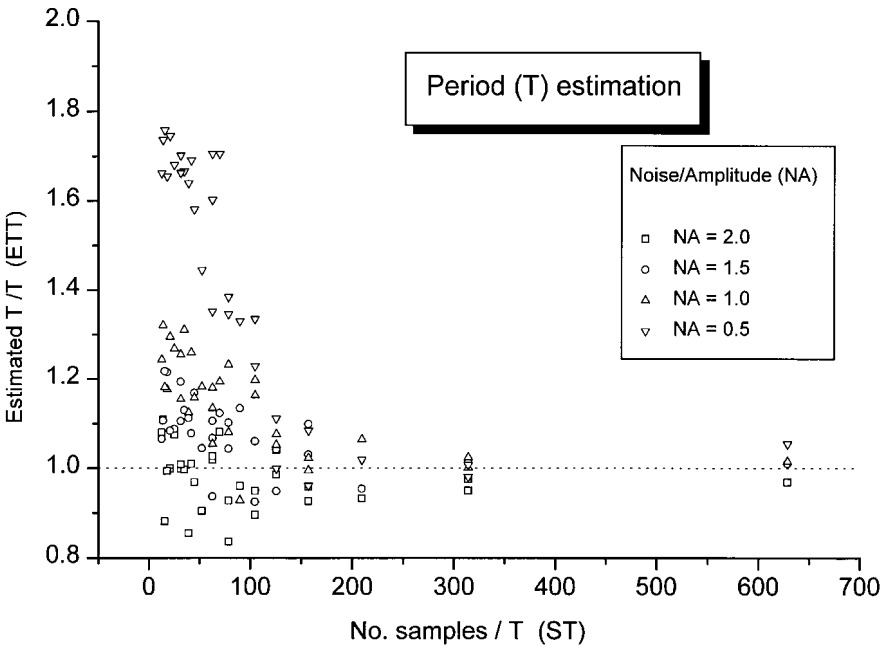

Figure 13. Simulation to test the algorithm's ability to reveal existing periodic components. Estimation of the original period of higher-order roughness. The dotted line represents the perfect agreement between simulated and estimated period

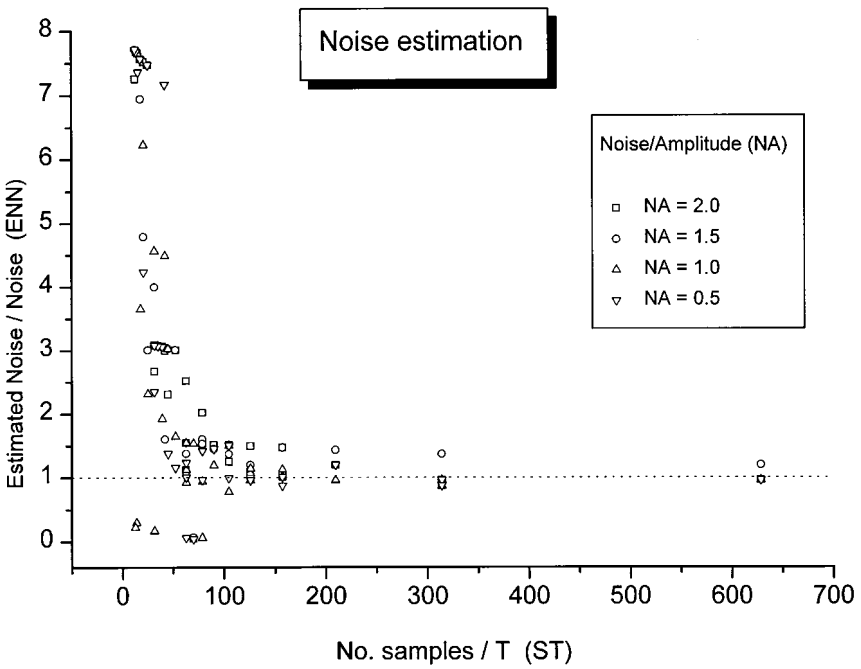

Figure 14. Simulation to test the algorithm's ability to reveal existing periodic components. Estimation of the original noise superimposed over original higher order roughness. The dotted line represents the perfect agreement between simulated and estimated noise.

the separate zones where the algorithm is able to detect (without appreciable error) the original period and noise in separate components. The zone where this capability is insufficient corresponds to the zone where the original signal is degraded because of sampling lag increase. The method is unable to detect the original period when ST values are lower than 100, irrespective of the NA values. The detection of original noise values, superimposed over the original profile with periodic properties, fails when the ST values are lower than 150 (Figure 14).

DISCUSSION

The proposed procedure divides the profile into a set of separate parts following a heuristic approach similar to the methods used in the analysis of a non-stationary time series, like the subdivision into small subseries with constant lengths considered as independent of one another as to periodograms and variance. The main characteristic of the proposed algorithm is the possibility of subdividing the profile avoiding predefined lengths and number of partitions. Consequently the partition lengths obtained depend on the local statistical properties. This approach greatly reduces the intrinsic subjectivity that remains only in the selection of segmentation criteria using the *Tfunction*s listed in Table II.

This kind of subjectivity is a disadvantage that is partly overcome by the kind of work done or by the kind of information retrieved from a profile. The examples in the paper are useful to explain the importance of the segmentation criteria. Table II shows the various *Tfunction*s corresponding to the different criteria of segmentation employed to analyse the examples from the S. Gimignano and Vicarello sites. Each *Tfunction* is suited to specific profile characteristics. The S. Gimignano profiles are analysed with SMALL-SLOPE criteria. This *Tfunction* was revealed to be most suitable where a major change in elevation is encountered and when greater detail in local slope trend was achieved.

SLOPE *Tfunction* used in Vicarello 2 and Vicarello 3 is more suitable for local slope trend analysis and local trend removal, with less detail with respect to the SMALL-SLOPE criteria. The AVERAGE criteria, used in Vicarello 1 profile, is more suited for profiles with no general slope trend.

In most of the slope-base cases the criteria (SLOPE and SMALL-SLOPE) remain most versatile because they are better able to extract the local slope trend that affects most profiles.

The remaining criteria (STDDEV and NONE), not exemplified here, have special properties. NONE criteria simply accumulate the elevations along the profile. These criteria have effects similar to the AVERAGE but are sometimes more effective because of their ability to scan and concentrate on small irregularities. Theoretically STDDEV should be ideal to detect local zones where standard deviations of elevation are quite constant. But these criteria are effective only on previously detrended profiles.

The calculation of a series of statistical parameters on the previously segmented profile offers additional information. Clear examples are given in Figures 7, 8, 9, 10 and 11. The random roughness superimposed over the local trend is obtained as the standard deviation of the local residues. Other additional information may be the local angle of the slope, or, as ib Figure 6, the AF index.

An interesting characteristic of the segmentation algorithm is the possibility of identifying the spatial distribution of some statistical properties of the surface and the existing pattern (Figures 6, 7c, 8c, 9c, 10c and 11c). The statistical distribution of the roughness index and other parameters in the profile, expressed in terms of a CDF, may be obtained by rearranging the frequency of a given parameter using its relative length with respect to the entire profile. The CDF may be successively used to determine the mean value or the most representative interval of confidence for the examined parameter. The CDF may be used for comparative studies of profiles without using a single statistical or roughness index (Figure 12).

Moreover, this representation makes for a better description and consequent reconstruction of the surface.

Several of the previously cited authors consider the roughness features a matter of scale of observations or, in other terms, they depend on the scale of the process that generates them and on the sampling interval length. This is a general concept that goes beyond the basic definition of 'oriented roughness' given previously.

The definition of oriented roughness presupposes the existence of some kinds of periodicity in higher-order roughness due to tillage so that a kind of 'order' exists rather than purely chaotic roughness.

A more general view of roughness may be based on a simple concept. Every lower order of roughness may be considered as random roughness of the closer higher-order roughness. In this way each order of roughness may be called 'ordered roughness' (OR) in relation to the closer and lower order of random roughness. This definition seems more suitable to study the presence of several components of roughness in the same profile, especially when the relative importance of each component is not constant along the profile. Each component extracted may be further analysed with the segmentation algorithm, and its own spatial structure and properties identified.

As observed from several authors, the profile-sampling step has a considerable influence on the final statistical parameters derived. The proposed algorithms are limited in the same way. The simulation described above on synthetic profiles shows how the limit to revealing previously known periodicity and noise is influenced by sampling lag and how a minimum density of points has to be achieved.

A sophisticated spectral analysis makes it possible to derive valuable information but not to evaluate local slope and the local storage capacity which may be evaluated by the knowledge of the local value of the RR index and slope by empirical relationship (Onstad, 1984) . In the same way a strong general trend filtering the original profile (linear or polynomial) can mask some higher-order roughness that produces effective water storage. Following this logic, a roughness profile has to be studied at the different scales that original sampling resolution allow so that all the information content may be available for appropriate uses.

A partial disadvantage of the method is the computational time because the algorithm is iterative in nature. The computation time depends mainly on the chosen *T-function*, the number of points in the profiles and also on the complexity of the profile's pattern. The present study indicates that the time of

computing remains acceptable when the number of points does not exceed 1500, but these problems may be partially overcome with future algorithm optimization work.

The proposed algorithm suggests several fields of possible applications such as the study of the differential evolution of the single roughness domains following hydrologic history of the soil, the study of the distribution of local aspect and slope inside a profile, the study of longitudinal distribution of surface storage related to local roughness properties, and finally as a general tool to study any other type of spatial series in a heuristic way.

CONCLUSIONS

The method described is introduced as a robust and flexible tool to study spatial series such as soil roughness profiles, that cannot be assumed to be stationary. Using an appropriate set of statistical functions (*Tfunction*s) that implement various segmentation criteria, local statistical and roughness properties are investigated. The proposed approach avoids using a classical spectral analysis but it assumes intrinsic non-stationary properties, thus making it possible to increase the information content that can be retrieved from a profile: spatial and statistical distributions of local roughness indexes or geometrical properties, and extraction of the local roughness components, random or non-random.

The procedure proposed may investigate, with various degrees of accuracy, the local properties of roughness and should be useful in monitoring the differential evolution of roughness on patterned soil surfaces, thus increasing information content.

Sampling distance of the roughness profile affects the algorithm's ability to reveal the roughness components. This behaviour is common to other methods because the signal degradation due to sampling lag determines the information content to process. In this case an initial attempt to evaluate the limits of the algorithm is made by giving the adimensional parameters that link sampling lag to the dimension of roughness components to be revealed.

The proposed definition of 'ordered roughness' seems more suitable for the current techniques of numerically processing digital profiles and for the existing physical relationships between the scale of roughness observation and the scale of the process investigated (hydraulic resistance, water storage depressions).

The approach of assuming the profile to be composed of independent domains has promising applications such as: the possibility to study the differential evolution of the single domains of roughness following hydrologic history of the soil; the study of the distribution of local aspect and slope inside a profile; the study of longitudinal distribution of surface storage related to local roughness properties; and as a general tool to study any other type of spatial series in a heuristic way.

ACKNOWLEDGEMENTS

The author especially acknowledges D. Torri, of the Institute for Soil Genesis and Ecology (CNR-IGES) for his invaluable help in critically reading and offering suggestions during the preparation of this manuscript.

REFERENCES

Allmaras, R. R., Burwell, R. E., Larson, W. E., Holt, R. F. and Nelson, W. W. 1966. *Total porosity and random roughness of the interrow zone as influenced by tillage,* USDA Conservation Research Report No. **7**, USDA-ARS, Washington, DC.

Andrle, R. and Abrahams, A. 1989. 'Fractal techniques and the surface roughness of talus slopes', *Earth Surface Processes and Landforms,* **14**, 197–209.

Bertuzzi, P., Caussignac, J. M., Stengel, P., Morel, G., Lorendeau, J. Y. and Pelloux, G. 1990a. 'An automated noncontact laser profile meter for measuring soil roughness in situ,' *Soil Science,* **149**(3), 169–178.

Bertuzzi, P., Rauws, G. and Corrault, D. 1990b. 'Testing roughness indices to estimate soil surface roughness changes due to simulated railfall,' *Soil and Tillage Research,* **17,** 87–99.

Brough, D. L. and Jarret, A. R. 1992. Simple technique for approximating surface storage of slit-tilled fields,' *Transactions of the ASAE,* **35**(3), 885–890.

Burwell, R. E., Allmaras, R. R. and Amemyia, M. 1963. 'A field measurement of total porosity and surface microrelief of soil,' *Soil Science Society of America Proceedings,* **27,** 697–700.
Currence, H. D. and Lovely, W. G. 1970. 'The analysis of Soil surface roughness,' *Transactions of the ASAE,* **13,** 710–714.
Destain, M. F., Descornet, G., Roisin, C. and Frainkinet, M. 1989. 'Investigation of soil degradation by means of an opto-electronic microreliefmeter,' *Soil and Tillage Research,* **13,** 299–315.
Dexter, A. 1977. 'Effect of rainfall on the surface micro-relief of tilled soil,' *Journal of Terramechanics,* **14**(1), 11–22.
Frede, H. and Gath, S. 1995a. 'Soil surface roughness as result of aggregate size distribution 1. 'Report: measuring end evaluation method,' *Z. Pfanzenernahr. Bodenk.,* **158,** 31–35.
Frede, H and Gath, S. 1995b. 'Soil surface roughness as result of aggregate size distribution 2. Report: Change in aggregate size classes caused by erosive rainfall,' *Z. Pfanzenernarh. Bodenk.,* **158,** 37–41.
Gallart, F. and Pardini, G. 1996. 'Perfilru: un programa para el analisis del la rugosidad de perfiles microtopograficos mediante el estudio de la geometria fractal,' Grandal d'Anglande, A. and Pages Valcarios, J. (Eds), *IV Reunion de Geomorfologia*, Sociedad Espanola de geomorfologia, O Castro (A Coruna), 164–176.
Gilley, J. E. and Finkner, S. C. 1991. 'Hydraulic roughness coefficients as affected by random roughness,' *Transactions of the ASEA,* **34**(3), 897–903.
Green, R. 1967. 'The spectrum of a set of measurements along a profile,' *Engineering Geology,* **2**(3), 163–168.
Hegge, B. J. and Masselink, G. 1996. 'Spectral analysis of geomorphic time series: auto-spectrum,' *Earth Surface Processes and Landforms,* **21**, 1021–1040.
Huang, C., White, I., Thwaite, E. G. and Bedeli, A. 1988. 'A noncontact laser system for measuring soil surface topography,' *Soil Science Society of America Journal,* **2,** 350–355.
Huang, C. and Bradford, J. M. 1992. 'Application of a laser scanner to quantify soil microtopography,' *Soil Science Society of America Journal,* **54,** 1402–1406.
Kuipers, H. 1957. 'A reliefmeter for soil cultivation studies,' *Netherlands Journal of Agricultural Science,* **5,** 255–262.
Lehrsch, G. A., Wishler, F. D. and Romkens, M. J. M. 1988. 'Selection of a parameter describing Soil Surface Roughness,' *Soil Science Society of America Journal,* **52,** 1439–1445.
Linden, D. R. and Van Doren, D. M. 1986. 'Parameters for characterising tillage induced soil surface rughness,' *Soil Science Society of America Journal,* **52,** 1439–145.
Linden, D. R., Van Doren, D. M., Allmaras, R. R. 1988. 'A model of the effect of tillage-induced soil surface roughness on erosion,' *ISTRO, 11th International Conference Proceedings, Tillage and Traffic in Crop Production,* 373–378.
Onstad, C A. 1984. 'Depressional storage on tilled soil surfaces,' *Transactions of the ASAE,* **27**(3), 729–732.
Perfect, E. and Kay, B. D. 1995. 'Application of fractals in soil and tillage research: a review,' *Soil and Tillage Research,* **36,** 1–20.
Pini, R., Pardini, G., Barbini, A., Raffaelli, M. E. and Vigna Guidi, G. 1995. 'Tecniche non invasive a luce laser nello studio delle alterazioni superficiali dei terreni, in Convegno *Il ruolo della pedologia nella pianificazione e gestione del territorio*, Cagliari, Italy.
Podmore, T. H. and Huggins, L. F. 1980. 'Surface roughness effects on overland flow,' *Transaction of the ASAE,* **23**, 1434–1439, 1445.
Poesen, J. 1988. 'Surface sealing on sandy and loamy soils: some aspects of seal formation and the influence of sealing on water erosion subprocesses,' *Quaderni del Scienza del Suolo,* CNR-Florence, **1,** 9–19.
Potter, K. N. 1990. 'Soil properties effect on random roughness decay by rainfall,' *Transaction of the ASAE,* **33**(6), 1889–1892.
Press, W. H., Flannery, B. P., Teukolsky, S. A. and Vetterling, W. T. 1986. *Numerical Recipes in Pascal,* Cambridge University Press, Cambridge.
Romkens, M. J. M. and Wang, J. Y. 1986. 'Effect of tillage on surface roughness,' *Transactions of the ASAE,* **29**(2), 429–433.
Romkens, M. J. M. and Wang, J. Y. 1987. 'Soil roughness changes from rainfall,' *Transactions of the ASAE,* **30**(1), 101–107.
Stone, R. O. and Dugundji, J. 1965. 'A study of microrelief – its mapping, classification, and quantification by means of a Fourier analysis,' *Engineering Geology,* **1**(2), 89–187.
Torri, D. 1996. 'Slope, aspect and surface storage,' in Agassi, M. (Ed.), *Soil Erosion, Conservation and Rehabilitation,* Marcel Dekker, New York.
Van Wesmael, B., Poesen, J., De figueriredo, T. and Govers, G. 1996. 'Surface roughness evolution of soil containing rock fragments,' *Earth Surface Processes and Landforms,* **21,** 399–411.
Whitehouse, D. J. 1994. *Handbook of Surface Metrology,* Institute of Physics Publishing, Bristol. 998pp.
Zobeck, T. M. and Onstad, C. A. 1987. 'Tillage and rainfall effects on random roughness: a review,' *Soil and Tillage Research,* **9,** 1–20.

